Synthesis and magnetic properties of $Zn_{1-x}Co_xO$ nanorods

L. W. Yang, X. L. Wu,[a] and T. Qiu
National Laboratory of Solid State Microstructures, Department of Physics, Nanjing University, Nanjing 210093, People's Republic of China

G. G. Siu and Paul K. Chu
Department of Physics and Materials Science, City University of Hong Kong, Kowloon, Hong Kong, China

(Received 18 July 2005; accepted 15 February 2006; published online 6 April 2006)

Magnetic $Zn_{1-x}Co_xO$ nanorods were fabricated via direct hydrothermal synthesis. The measurements of x-ray diffraction, x-ray photoemission spectroscopy, and optical absorption spectra demonstrate the presence of cobalt in the +2 state in a tetrahedral crystal field, which indicates that Co ions have been doped into the nanorods. The observations of morphology and microstructure reveal that the $Zn_{1-x}Co_xO$ nanorods grow along the [0002] direction through Ostwald ripening not only competing with but being assisted by oriented attachment. The field dependence of magnetization (*M-H* curves) of the $Zn_{1-x}Co_xO$ nanorods measured at 300 K shows their ferromagnetic characteristics. The coercive fields (H_c) were obtained to be 98 and 36 Oe for nominal $x=0.029$ and 0.056, respectively. Our experimental results provide one effective method for fabrication of transition metal doped ZnO nanostructures with room-temperature ferromagnetism by direct chemical synthesis. © *2006 American Institute of Physics*. [DOI: 10.1063/1.2188031]

I. INTRODUCTION

Diluted magnetic semiconductors (DMSs) have attracted a lot of attention for their potential applications in the field of spin-dependent semiconductor electronics or so-called spintronics. A key work to realizing spintronic devices is to develop DMSs with room-temperature ferromagnetism. As one of the II-VI compound semiconductors, ZnO has attracted much interest because recent theory predicted the existence of room-temperature ferromagnetism of some semiconducting ZnO materials doped with suitable magnetic ions.[1,2] Subsequently, several transition metal (TM)-doped ZnO films, including Co-, V-, and Fe-doped and Co- and Fe-codoped ZnO films,[3–6] were reported to have the Curie temperature higher than 300 K. Nanoscale DMSs, including quantum dots, quantum wells, and quantum wires, are envisioned as pivotal architectural elements in several spintronics devices.[7] Spin effects in nanoscale semiconductors are still largely unexplored, however, and many essential advances in this field would be facilitated by the development of facile methods for the preparation of high-quality DMS nanostructures. In order to obtain magnetic nanostructures, ion implantation was previously employed to introduce Mn and Co into ZnO nanobelts and nanorods.[8,9] Recently Wu *et al.*[10] prepared $Zn_{1-x}Co_xO$ nanorods by *in situ* doping of Co in ZnO nanorods using a simple chemical vapor deposition (CVD) method and observed ferromagnetism with a Curie temperature higher than 350 K. Solution chemical synthesis, including microemulsion and hydrothermal growth, has also proven effective and convenient in preparing ZnO nanowires, nanorods, and helical rods at low temperature.[11–13] These successes have motivated us to explore the possibility of solution-based synthetic routes for preparation of one dimensional (1D) TM-doped ZnO nanostructures. Direct chemical syntheses of ZnO DMSs may allow better control over chemical composition and dopant speciation than ion implantation technique and CVD methods. Furthermore, solution chemical synthesis offers attractive advantages for scaling up and processing production, compared with other synthetic methods. Unfortunately, few reports have been presented on fabrication of 1D TM-doped ZnO nanostructures with room-temperature ferromagnetism by direct chemical synthesis. In this work, we fabricate $Zn_{1-x}Co_xO$ nanorods through direct hydrothermal synthesis and characterize the structural and magnetic properties of the Co-doped ZnO nanorods.

II. SAMPLES AND EXPERIMENTS

Co-doped ZnO nanorods were synthesized by a hydrothermal method which was similar to that reported by Liu and Zeng.[13] In a typical preparation, 2.934 g zinc nitrate $[Zn(NO_3)_2 \cdot 6H_2O]$, 11.2 g KOH, and the required amount of cobalt nitrate $[Co(NO_3)_2 \cdot 6H_2O]$ were dissolved in de-ionized water to form a 20 ml solution. In this process, we found that the solution color turns from initial pink into blue with addition of KOH. Then 3 ml of the above solution was mixed with 5.0 ml de-ionized water and 25.0 ml pure alcohol (C_2H_5OH), followed by adding 5.0 ml ethylene diamine $[C_2H_4(NH_2)_2]$. Before being transferred to a Teflon-lined autoclave with an internal volume of 25 ml, the solution mixture was pretreated under an ultrasonic water bath for 45 min. The hydrothermal syntheses were conducted in an electric oven at 175 °C for 20 h. After the reactions, the obtained blue-green products were harvested by centrifugation and thorough washing with de-ionized water, and finally dried at 40 °C for 24 h.

The crystal structures and the Co doping concentrations of the obtained samples were determined by x-ray diffraction

[a]Author to whom correspondence should be addressed; electronic mail: hkxlwu@nju.edu.cn

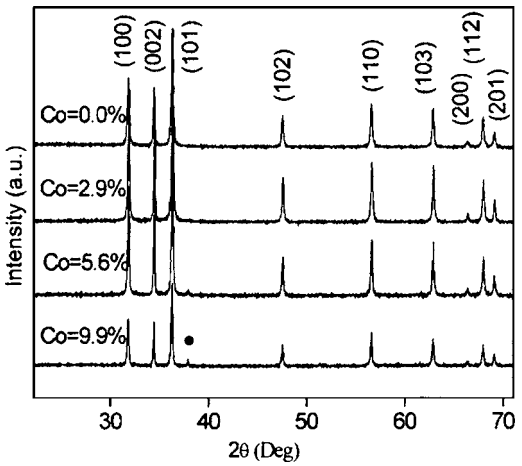

FIG. 1. Typical powder XRD patterns of the $Zn_{1-x}Co_xO$ nanorods with nominal Co doping concentrations of $x=0$, 0.029, 0.056, and 0.099, respectively.

(XRD) measurements using the Cu $K\alpha$ radiation and inductively coupled plasma (ICP J-A1100) analysis. The morphologies and microstructures of the synthesized samples were characterized using field emission scanning electron microscopy (SEM) equipped with an EDAX PV7715/89 ME energy dispersive x-ray spectrometer (EDXS) and high-resolution transmission electron microscopy (HRTEM, FEI Tecnai G^2 20 S-TWIN) equipped with selected area electron diffraction (SAED). Optical absorbance measurements were performed at room temperature using an ultraviolet-visible spectrometer (Lambda900). The obtained samples were also characterized by x-ray photoemission spectroscopy (XPS, ESCALB MK-II) using Al K radiation ($h\upsilon=1486.6$ eV). The magnetic properties of the samples were investigated using a superconducting quantum interference device magnetometer (SQUID, MPMS XL-7).

III. RESULTS AND DISCUSSIONS

Figure 1 shows some typical powder XRD patterns of the $Zn_{1-x}Co_xO$ nanorods with nominal Co doping concentrations of $x=0\%$, 0.029%, 0.056%, and 0.099% (the actual Co contents of the as-prepared samples were determined by ICP analysis, as shown in Table I). These XRD patterns show that no other impurity phases exist for nominal doping concentrations below 5.6%. The Co doping does not change wurtzite structure of ZnO. With increasing Co doping concentration above 5.6%, the diffraction pattern displays a weak undesired peak (labeled by ●) at 37.9°, which corresponds to the (101) diffraction peak of $Co(OH)_2$. The lattice parameters calculated from the XRD data demonstrate that their values are close to but slightly smaller than those of pure ZnO (see Table I). In addition, it is noticeable that the variation of the lattice parameters with Co concentration is not monotonic. The two results above are understandable, because the effective ionic radius (0.58 Å) of Co^{2+} in tetrahedral configuration is close to that of Zn^{2+} (0.60 Å).[14,15]

TABLE I. Nominal Co concentrations in the reaction mixture, the Co concentrations determined by both ICP and EDX analyses, and the lattice constants calculated according to the XRD data.

Co% nominal		0.0	2.9	5.6	9.9
Co% ICP analysis		0.0	1.42	3.57	5.86
EDX analysis		0.0	1.71	5.07	7.82
Calculated lattice	a	3.258	3.254	3.254	3.255
Constant (Å)	c	5.217	5.213	5.211	5.214

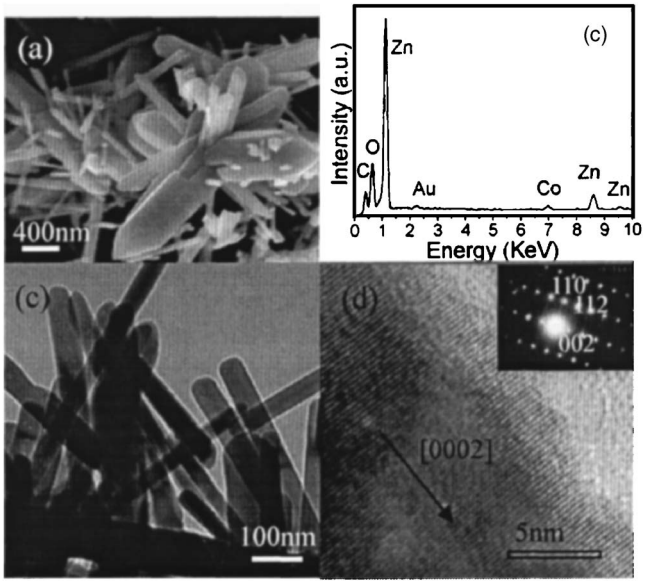

FIG. 2. (a) Typical SEM images of the $Zn_{1-x}Co_xO$ nanorods with nominal Co concentration of $x=0.029$. (b) EDXS results of a bundle of nanorods with nominal Co concentration of $x=0.029$. (c) A low-magnified TEM image of the $Zn_{1-x}Co_xO$ nanorods. (d) A HRTEM image of a $Zn_{1-x}Co_xO$ nanorod with the corresponding SAED pattern inserted. The SAED pattern was taken with an electron beam along the [100] zone axis.

Figure 2(a) shows a typical SEM image of the $Zn_{1-x}Co_xO$ nanorods with nominal $x=0.029$. It can be seen that the synthesized material is a mixture of nanorods with different diameters ranging from 50 to 400 nm. However, we can find that most nanorods have a uniform diameter along their entire lengths, indicating that the growth anisotropy in the $+c$ axis is strictly maintained throughout growth process. Figure 2(b) is a typical EDXS pattern obtained from a bundle of nanorods. Quantitative analysis reveals that the atomic composition ratio of $(Zn_{1-x}Co_x):O$ is about 1:1 and the amount of Co incorporated into the nanorods is slightly more ($x=0.017$) than half of the nominal amount of Co added during the synthesis, which matches with the ICP analysis.

The morphology and microstructure of the $Zn_{1-x}Co_xO$ nanorods were further examined by TEM observations. Figure 2(c) shows a typical low-magnified TEM image. It can be found that most nanorods are straight in morphology and smooth in surface. Figure 2(d) shows a high-resolution TEM image and its inset shows the SAED pattern of a single $Zn_{1-x}Co_xO$ nanorod. The lattice fringes can be clearly seen in the HRTEM image, revealing that the nanorod is single crystalline. Lattice spacing d between any two adjacent lattice fringes is 0.261 nm, which matches that of the (0002) plane of wurtzite structural ZnO, indicating that the nanorod grows along the [0002] direction. We also examined the HRTEM images of different regions of a nanorod and found that no segregated impurity phase exists throughout the nanorod. In

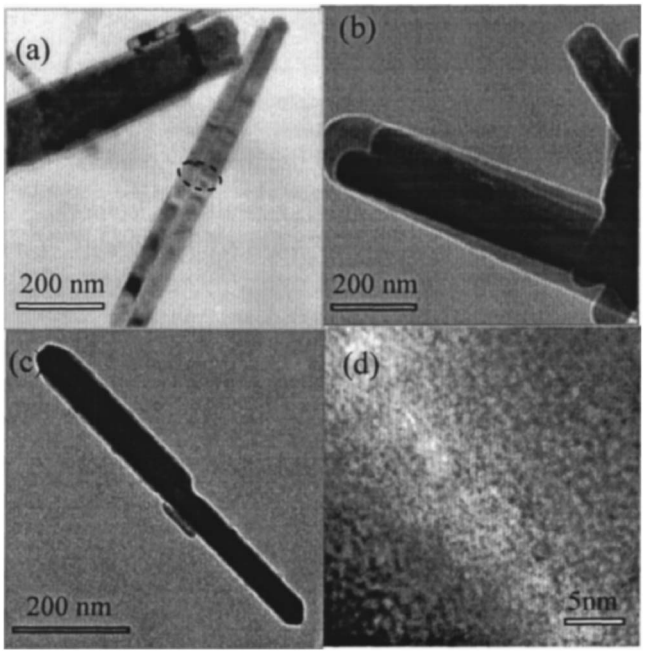

FIG. 3. (a) Typical TEM image of two nanorods attaching together parallel to the *c* axis. (b) Typical TEM image of two nanorods attaching together vertical to the *c* axis. (c) Three nanorods attaching together to form a big one. (d) The corresponding HRTEM image of the area marked by a circle in (a). Central lighter areas are the boundaries between two nanorods.

particular, a small number of detached nanorods undergoing a multiplying growth via "oriented attachment"[13,16–18] (a large crystal is formed by direct combination of several small crystals) can be observed in our samples, as shown in Figs. 3(a)–3(c). These figures clearly show two or three nanorods attaching together to form a large nanorod. The HRTEM image of the area marked by a circle in Fig. 3(a) displays perfect lattice continuity of the two attached nanorods [see Fig. 3(d)].

Figure 4(a) shows the optical absorption spectrum of the as-prepared $Zn_{1-x}Co_xO$ nanorods with a nominal Co concentration of $x=0.029$. Three characteristic absorption peaks can be observed around 565, 612, and 657 nm, respectively. These peaks relate to the *d-d* transitions of the tetrahedrally coordinated Co^{2+} ions and can be attributed to the $^4A_2(F) \rightarrow {}^2E(G)$, $^4A_2(F) \rightarrow {}^4T_1(P)$, and $^4A_2(F) \rightarrow {}^2A_1(G)$, respectively. This result indicates that Co ions have been at the lattice positions of Zn ions and in a tetrahedral crystal field in the +2 state.[19] Figure 4(b) presents the Co $2p$ core level XPS spectrum of the Co-doped samples. The charge-shifted spectra were corrected using the maximum of the adventitious C $1s$ signal at 284.6 eV. The Co $2p_{3/2}$ peak occurs at 780.48 eV, while the Co $2p_{1/2}$ peak is located at 796.2 eV. The difference between Co $2p_{1/2}$ and $2p_{3/2}$ is 15.8 eV, showing large chemical shifts compared to that of pure Co metal (15.05 eV). This indicates that Co ions have a 2+ valence in a rather high probability.[20] Satellite peaks also appear at about 786.5 and 802.6 eV, respectively, which originate from the charge-transfer band structure characteristic of the $3d$ transition metal monoxides.[21] The differences between the main peaks and the corresponding satellites further prove

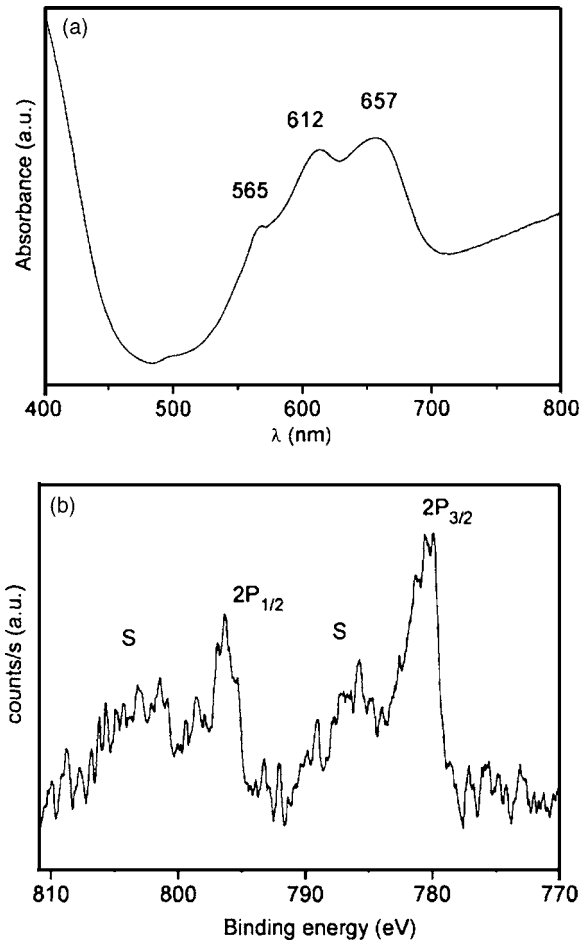

FIG. 4. (a) Room-temperature optical absorbance spectrum of the $Zn_{1-x}Co_xO$ nanorods with nominal Co concentration of $x=0.029$. (b) The corresponding Co $2p$ core level XPS spectrum. Label "S" denotes the satellite peaks.

that Co ions are in a tetrahedral crystal field surrounded by oxygen atoms and have a chemical valence of the +2 state.

The growth habit of polar ZnO crystal under hydrothermal condition has been investigated by many researchers and it has been revealed that 1D growth along the [0002] direction of ZnO nanostructure is related to both its intrinsic crystal structure (intermolecular bonding preferences or dislocations) and external factors (supersaturation, temperature, solvents, impurities, etc.). Besides traditional Ostwald ripening, another growth mechanism, oriented attachment, has been proposed for the anisotropic growth of ZnO nanostructures in recent years.[16] In our case, we found that Co impurities have less influence on the growth of ZnO nanorods compared with that of internal pressure of autoclave, solvents, and the ultrasonic pretreatment of the solution mixture. Therefore, we focus on how Co impurities are incorporated into the ZnO nanorods. Recently, Schwartz *et al.*[22] have prepared Co-doped ZnO nanocrystals using direct chemical routes. Their spectroscopic measurements disclosed that there are no Co^{2+} ions in the initially nucleated ZnO cores and that Co^{2+} ions in solution remained octahedrally coordinated until the nucleation of ZnO crystallites, at which point they bind to the nanocrystal surfaces in tetrahedral geometries either as monomers or within basic acetate clusters,

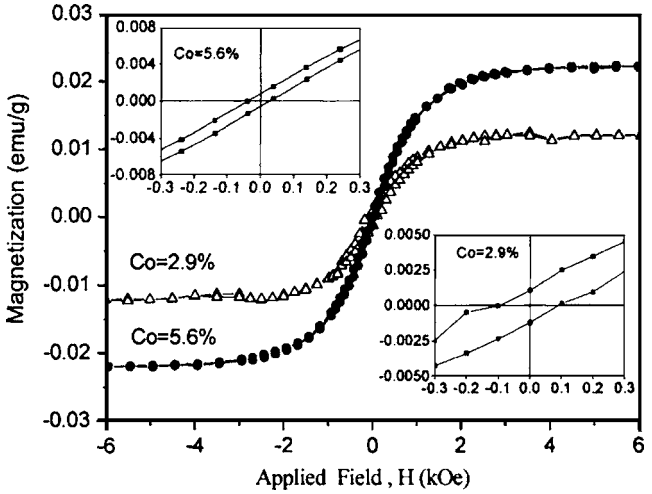

FIG. 5. *M-H* curves of the $Zn_{1-x}Co_xO$ nanorods with nominal Co doping concentrations of $x=0.029$ and 0.056 detected at 300 K. The insets show two magnified portions of the *M-H* curves near the centers.

and subsequent reaction with OH^- yields substitutionally Co^{2+} doping in ZnO. According to the experimental observation, we consider that the Co^{2+} ion is incorporated into ZnO nanocrystals through similar approach because the change of solution color is similar to that reported by Schwartz *et al.* before hydrothermal reaction. Further combining with our TEM observations, we consider that these Co-doped ZnO nanocrystals follow to grow along the [0002] direction to yield finally high-quality $Zn_{1-x}Co_xO$ nanorods through Ostwald ripening not only competing with but being assisted by oriented attachment under hydrothermal condition.

Figure 5 presents the *M-H* curves (field dependence of magnetization) of the $Zn_{1-x}Co_xO$ nanorods with nominal Co concentrations of $x=0.029$ and 0.056 detected at 300 K. The diamagnetic contribution from the sample holder has been subtracted from the data. Hysteresis loops can be observed at 300 K, showing obvious ferromagnetic characteristics. The coercive fields (H_c) are obtained to be 98 and 36 Oe (see the insets) for $x=0.029$ and 0.056, respectively. Saturation magnetizations of 0.0125 and 0.0221 emu/g at 5 kOe can be observed for $x=0.029$ and 0.056, respectively. With increasing Co concentration, H_c decreases. This is similar to the results reported by Yin *et al.*[20] in Co-doped ZnO films. In fact, no hysteresis loop was observed in the *M-H* curves of the sample with nominal Co concentration of $x=0.099$ (not shown here). There are two possible origins of the ferromagnetism in the $Zn_{1-x}Co_xO$ system. They are magnetic Co precipitations and carrier induced ferromagnetism.[19,23] According to our results of XRD, HRTEM, XPS, and optical absorption spectra, the possibility of Co precipitations can be ruled out. Since ferromagnetism in the $Zn_{1-x}Co_xO$ nanorods originates from the exchange interaction between free delocalized carriers (hole or electron from the valence band) and the localized *d* spins on the Co ions, the presence of free carriers is a necessary condition for the appearance of ferromagnetism. Free carriers can be induced by doping, defects, or Co ions in another oxidation state such as Co^{3+}. Recently, Kittilstved *et al.*[24] have reported the use of *ex situ* targeted *p*- and *n*-type chemical perturbations to manipulate high-T_C (Curie temperature) ferromagnetism in Mn-doped and Co-doped ZnO nanocrystal films. On this basis, it can be concluded that in our $Zn_{1-x}Co_xO$ nanorods with increasing Co doping concentration, the free carriers should decrease and the dominant magnetic interaction between Co^{2+} ions becomes nearest-neighbor antiferromagnetic. As a result, room-temperature ferromagnetism gradually disappears. Further investigation on the magnetic property and its origin of $Zn_{1-x}Co_xO$ nanorods is currently in progress.

So far, it is still unclear whether these reported synthetic routes in Refs. 11–13 can be extended to prepare 1D TM-doped ZnO nanostructures and how the impurities are incorporated into the ZnO nanostructures, because the impurities would have great influence on the growth of ZnO nanostructures. At this point, our experimental results provide an effective method for fabricating the TM-doped ZnO nanostructures with room-temperature ferromagnetism under "one-pot conditions" (*direct chemical synthesis*). Although the ferromagnetism in our current $Zn_{1-x}Co_xO$ nanorods via our synthetic route remains relatively weak, unambiguous observation of the ferromagnetism is of scientific significance and technological value. Recently, Cui and Gibson[25] reported that the ZnO nanostructures without TM doping can be prepared through the synthetic route described in Ref. 12, under the condition without any modification. This is an important progress in sample fabrication.

IV. CONCLUSIONS

We have synthesized the $Zn_{1-x}Co_xO$ nanorods through direct hydrothermal synthesis. The measurements of XRD, XPS, optical absorption spectra, and HRTEM demonstrate that Co ions have been doped into the nanorods. The SEM and TEM observations reveal that the $Zn_{1-x}Co_xO$ nanorods grow along the [0002] direction through Ostwald ripening not only competing with but being assisted by oriented attachment. The *M-H* curves of the $Zn_{1-x}Co_xO$ nanorods show their ferromagnetic characteristics at 300 K and the coercive fields (H_c) are 98 and 36 Oe for $x=0.029$ and 0.056, respectively. Although it remains challenging to utilize ferromagnetic $Zn_{1-x}Co_xO$ nanorods for practical applications due to their relatively weak ferromagnetism, unambiguous observation of their ferromagnetism in our current nanostructure is of intense scientific and technological interest.

ACKNOWLEDGMENTS

This work was supported by Grant Nos. 10225416, 60476038, and 60421003 from the National Natural Science Foundation of China and the LAPEM. Partial support was also from the Major State Basic Research Project No. G2001CB3095 of China and Hong Kong Research Grants Council (RGC) Competitive Earmarked Research Grants (CERG) CityU 1137/03E, and City University of Hong Kong Direct Allocation Grant 9360110.

[1] T. Dietl, H. Ohno, F. Matsukura, J. Cibert, and D. Ferrand, Science **287**, 1019 (2000).
[2] K. Sato and H. Katayama-Yoshida, Physica E (Amsterdam) **10**, 251 (2001).
[3] K. Ueda, H. Tabata, and T. Kawai, Appl. Phys. Lett. **79**, 988 (2001).

[4]H. Saeki, H. Tabata, and T. Kawai, Solid State Commun. **120**, 439 (2001).
[5]S.-J. Han, J. W. Song, C.-H. Yang, S. H. Park, J.-H. Park, Y. H. Jeong, and K. W. Rhie, Appl. Phys. Lett. **81**, 4212 (2002).
[6]Y. M. Cho, W. K. Choo, H. Kim, D. Kim, and Y. E. Ihm, Appl. Phys. Lett. **80**, 3358 (2002).
[7]S. A. Wolf, D. D. Awschalom, R. A. Buhrman, J. M. Daughton, S. V. Molnár, M. L. Roukes, A. Y. Chtchelkanova, and D. M. Treger, Science **294**, 1489 (2001).
[8]K. Ip *et al.*, J. Vac. Sci. Technol. B **21**, 1476 (2003).
[9]C. Ronning, P. X. Gao, Y. Ding, and Z. L. Wang, Appl. Phys. Lett. **84**, 783 (2004).
[10]J.-J. Wu, S.-C. Liu, and M.-H. Yang, Appl. Phys. Lett. **85**, 1027 (2004).
[11]L. Guo, Y. L. Ji, H. Xu, P. Simon, and Z. Wu, J. Am. Chem. Soc. **124**, 14864 (2002).
[12]L. Vayssieres, Adv. Mater. (Weinheim, Ger.) **15**, 464 (2003).
[13]B. Liu and H. C. Zeng, J. Am. Chem. Soc. **125**, 4430 (2003).
[14]Y. Z. You, T. Fukumura, Z. Jin, K. Hasegawa, M. Kawasaki, P. Ahmet, T. Chikyow, and H. Koinuma, J. Appl. Phys. **90**, 4246 (2001).
[15]R. D. Shannon, Acta Crystallogr., Sect. A: Cryst. Phys., Diffr., Theor. Gen. Crystallogr. **32**, 751 (1976).
[16]C. Pacholski, A. Komowski, and H. Weller, Angew. Chem., Int. Ed. **41**, 1188 (2002).
[17]J. H. Yu, J. Joo, H. M. Park, S.-I. Baik, Y. W. Kim, S. C. Kim, and T. Hyeon, J. Am. Chem. Soc. **127**, 5662 (2005).
[18]K.-S. Cho, D. V. Talapin, W. Gaschler, and C. B. Murray, J. Am. Chem. Soc. **127**, 7140 (2005).
[19]S. Ramachandran, A. Tiwari, and J. Narayan, Appl. Phys. Lett. **84**, 5255 (2004).
[20]Z. G. Yin, N. F. Chen, C. L. Chai, and F. Yang, J. Appl. Phys. **96**, 5093 (2004).
[21]G. A. Garson, M. H. Nassir, and M. A. Langell, J. Vac. Sci. Technol. A **14**, 1637 (1996).
[22]D. A. Schwartz, N. S. Norberg, Q. P. Nguyen, J. M. Parker, and D. R. Gamelin, J. Am. Chem. Soc. **125**, 13205 (2003).
[23]J. H. Park, M. G. Kim, H. M. Jang, S. Ryu, and Y. M. Kim, Appl. Phys. Lett. **84**, 1338 (2004).
[24]K. R. Kittilstved, N. S. Norberg, and D. R. Gamelin, Phys. Rev. Lett. **94**, 147209 (2005).
[25]J. B. Cui and U. J. Gibson, Appl. Phys. Lett. **87**, 133108 (2005).